RSC Advances

PAPER

View Article Online
View Journal | View Issue

Cite this: *RSC Adv.*, 2021, **11**, 592

Aromatic nature of neutral and dianionic 1,4-diaza-2,3,5,6-tetraborinine derivatives†

Kei Ota and Rei Kinjo *

The aromatically relevant parameters of boron-rich inorganic benzenes—neutral and dianionic 1,4-diaza-2,3,5,6-tetraborinine derivatives ($B_4N_2R_6$)—have been computationally estimated and evaluated from geometric, electronic, magnetic, and energetic points of view. The majority of the criteria (ASE, $NICS_{zz}$, ELF, and PDI) indicate that the aromaticity of the neutral B_4N_2 benzene analogue stabilized by Lewis bases lies in between those of benzene and borazine. On the other hand, the aromaticity of the dianionic B_4N_2 benzene analogue **4′** is controversial. The pronounced aromatic nature of **4′** is supported by ELF_{π}, PDI, and $NICS_{\pi zz}$, but ASE, the FiPC-NICS plot, and ACID oppose this. These data confirm that even with the same B_4N_2-skeletal framework of a 6π-system, the aromatic feature varies depending on the overall charge of the B_4N_2 systems.

Received 23rd October 2020
Accepted 15th December 2020

DOI: 10.1039/d0ra09040a

rsc.li/rsc-advances

Introduction

Since the discovery of the cyclic feature of benzene $(CH)_6$ **1** in 1865, "aromaticity" has represented one of the most significant fundamental concepts in modern chemistry.[1–3] Nowadays, its implication is not limited to the molecules obeying the $[4n + 2]$ Hückel rule, but extended to those satisfying various criteria—structural, electronic, magnetic and energetic indices can be employed to assess the aromatic nature of a molecule comprehensively. It is well known that benzene **1**, an archetypal aromatic molecule, displays a planar geometry, cyclic delocalization of 6π electrons, peculiar magnetic properties and extra thermodynamic stability.[4,5]

Synthetically, incorporation of isolobal heteroatom units into the benzene scaffold is one of the useful strategies to modify the intrinsic electronic property of aromaticity without significant change of the geometric feature. Indeed, a variety of inorganic benzenes have been developed thus far,[6] most of which are mainly based on the $(XY)_3$ system, such as borazine $(HBNH)_3$ **2**, boroxines $(RBO)_3$ and phosphazenes $(R_2PN)_3$.[7–10] The six-membered ring aromatics based on heavier elements have little been described.[11–15]

Theoretically, the aromaticity of inorganic benzenes has been evaluated using computational methods such as nucleus-independent chemical shift (NICS), aromatic stabilization energies (ASE) and electron localization function (ELF) analyses.[16–26] In 1991, Fink and Richards reported the calculated ASE values of the $(XY)_3$ ring systems (X = BR, AlR; Y = NR, PR),[16] and revealed that the ASE values increase in order AlN < BN < BP < CC. In 1997, the group of Schleyer estimated the NICS values of the $(XY)_3$ rings (X = BH, AlH, CH; Y = NH, PH, O, S), as well as, the E_6 rings (E = SiH, GeH, N, P).[17] The NICS values of the $(XY)_3$ systems are found to be less negative than that of benzene whereas the E_6 systems are comparable to benzene. In 1998, Jemmis *et al.* systematically evaluated the aromaticity of the $(XY)_3$ molecules (X = BH, AlH, GaH, PH_2; Y = NH, PH, AsH, N, O, S, Se) using ASE, magnetic susceptibility exaltation (MSE), and NICS analyses. As a result, they concluded that judicious use of all criteria is needed in gauging aromaticity of those systems.[18] In 2005, Jenneskens and coworkers reported the electronic structure of the $(XY)_3$ (X = BH, AlH; Y = NH, PH, O, S) and E_6 (E = SiH, GeH, N, P) systems by using valence bond (VB) theory and ring-current maps. The authors unveiled that in general, the heteronuclear systems $(XY)_3$ show localization of the lone pair of electrons on the electronegative atoms, and Kekulé-like structures do not contribute.[19] In 2010, Phukan and Silvi *et al.* calculated the NICS, ASE, and ELF values for the substituted $(XY)_3$ systems (X = BR, AlR; Y = NH, PH, AsH, O, S, Se). The results clarified the substituent effect—the bulky electronegative substituents (*R*) on B or Al atoms dramatically increases the stability and aromaticity.[20] Recently, Alvarez-Thon and Tiznado examined the $(XYH)_3$ systems (X = C–Pb, Y = N–Bi) by magnetically induced current density (MICD) and the zz component of NICS, and revealed that most of them are aromatic except for $(XNH)_3$ (X = Si–Pb).[21]

The extant theoretical study on the aromaticity of inorganic benzenes mainly focuses on the above-mentioned $(XY)_3$ and E_6 systems, because those types of analogues have been isolated to date. Recently, we have reported the synthesis of a neutral B_4N_2-based benzene analogue, namely 1,4-diaza-2,3,5,6-tetraborinine derivative **3**,[27] being the first examples of the Lewis base-stabilized

Division of Chemistry and Biological Chemistry, School of Physical and Mathematical Sciences, Nanyang Technological University, 21 Nanyang Link, Singapore 637371, Singapore. E-mail: rkinjo@ntu.edu.sg

† Electronic supplementary information (ESI) available. See DOI: 10.1039/d0ra09040a

X_4Y_2 system.[6] Preliminary theoretical investigations including NICS, natural bond orbital (NBO), and anisotropy of the current-induced density (ACID) analysis suggested the pronounced aromatic nature of **3**. By contrast, the dianionic B_4N_2 ring system **4**: $[(Ph\text{-}N)_2(Me_2N\text{-}B)_4]^{2-}$ is found to furnish a non-aromatic twisted structure despite its 6π-electron configuration isoelectronic with **3**.[28] With the isolable neutral and dianionic B_4N_2 derivatives in hand, we wondered (i) how the aromatic nature of the B_4N_2 ring systems differs from the reported $(XY)_3$ systems, and (ii) whether the charge of molecules affects the aromaticity or not. Here, we have investigated the aromaticity of 1,4-diaza-2,3,5,6-*tetra*borinine derivatives, B_4N_2 analogues of benzene, by using modern computational aromaticity descriptors involving structure, molecular orbital, electron density, magnetic shielding, and energetics.[29] For purpose of comparison, reference molecules—benzene $(CH)_6$ **1**, and borazine $(HBNH)_3$ **2** have also been examined (Scheme 1). The substituent effect on the aromaticity in benzene as well as in borazine has been reported.[30–36] According to those prior studies, while the aromaticity of benzene resists substituent influences, that of borazine is significantly affected by the nature of substituents. In borazine, generally the electron-donating group (EDG) on B decreases the aromaticity, although electron-withdrawing group (EWG) on B and both EDG and EWG on N lead to the pronounced aromaticity. Therefore, we employed model compound **3′**, and a dianionic $B_4N_2H_6$ derivative **4′** (Scheme 1).

To evaluate the aromatic nature, five criteria including the harmonic oscillator model of aromaticity (HOMA), ELF, *para*-delocalization index (PDI), NICS, and ASE have been assessed.[16–20] Moreover, we have carried out ACID analysis to visualize the ring current.

Computational methods

All density functional theory calculations have been performed using the Gaussian 16 program package at the B3LYP/6-311+G(d,p) level,[37] which is widely employed for the estimation of aromaticity of monocyclic heterobenzenes and inorganic benzenes.[17,38–40] Note that when the basis sets as 6-311+G(2df,2pd) and 6-311+G(3df,3pd) in the optimization and NICS calculations for dianionic **4′** were employed, almost no significant improvement was observed (Table S2†). We used the NBO method in the current NBO 7.0 version of the general NBO analysis program.[41] PDI, ELF, and atoms in molecules (AIM) studies were generated with the Multiwfn 3.6 program.[42]

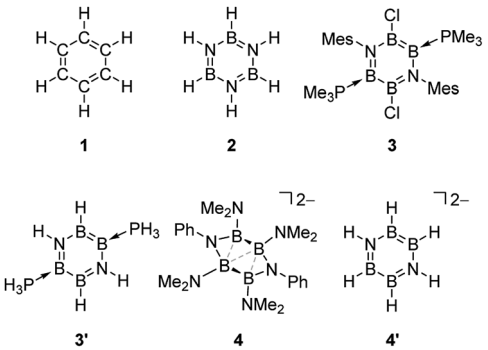

Scheme 1 The list of the molecules discussed in this article (Mes = 2,4,6-$Me_3C_6H_2$).

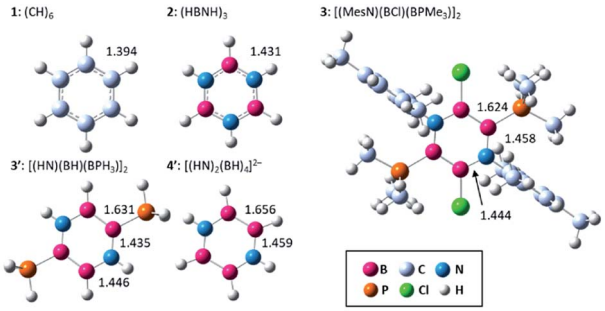

Fig. 1 Optimized structures and selected bond lengths (in Å) of **1**, **2**, **3**, **3′** and **4′**.

Results and discussion

Fig. 1 displays the optimized structures and selected bond lengths of benzene (**1**), borazine (**2**), and three B_4N_2 systems (**3**, **3′**, and **4′**). All molecular geometries were fully optimized as closed-shell species and characterized as energy minima by the absence of imaginary vibrational frequencies. The central six-membered ring in compounds **1**, **2**, **3** and **3′** exhibits a planar geometry. Notably, dianionic **4′** also bears a planar B_4N_2 ring, which is in stark contrast to the twisted ring framework experimentally observed for **4**, implying the impact of substituents at the B and N atoms on the skeletal geometry.[30,32–36] The selected π-type molecular orbitals (π-MOs) of **3′** and **4′** are summarized in Fig. 2. Three explicit π-MOs are seen in **3′** and **4′**, which are similar to those of benzene **1** and borazine **2**. While **1** and **2** have two degenerated highest occupied molecular orbitals (HOMOs), the B_4N_2 systems (**3**, **3′**, **4′**) possess non-degenerate π-MOs.[27] In the π-MOs of **3**, some contributions from 3p-orbitals of the substituents (Cl and PMe_3) are found. To assess the essential nature of the six-membered skeleton without consideration of the significant electronic perturbation from the substituent, **3** is omitted from NICSπ and ELFπ calculation (*vide infra*).

Firstly, a structural criterion is evaluated using the HOMA index, which is based on the equalization of the bond lengths and symmetry.[43–45] The calculated HOMA values, resonance energy (EN), and bond length alternation (GEO) are summarized in Table 1 (for the details of bond number, see Table S2†).[46,47] It should be noted that the HOMA index reflects only the geometrical features and does not consider the polarization effect on electronic distribution. Besides, HOMA values may depend on the choice of reference bond lengths and normalization constant. The reported constants of B–B and B–N bond are calculated in different way.[48,49]

The HOMA values increase in the order **4′** < **3′** < **3** < **1** ≈ **2**, from 0.288 for **4′** up to 1.000 for **2**. There is little bond alternation in **1** and **2**, in line with their essential D_{6h} and D_{3h} symmetries. For the B_4N_2 systems (**3**, **3′**, **4′**), both EN and GEO values are larger than those for benzene **1** and borazine

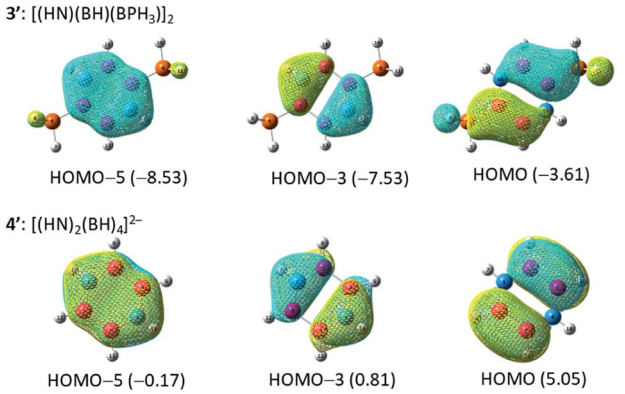

Fig. 2 Plots of the π molecular orbitals of **3′** and **4′** (in eV).

2. Particular diagnostic is that the HOMA value of **4′** is mainly dominated by EN term (0.428) rather than GEO term (0.284), indicating elongation of the skeletal bonds. The bond numbers of **3** [1.143 (B–B), 1.444–1.513 (B–N)], and **3′** [1.101 (B–B), 1.504–1.561 (B–N)] indicate partial bond alternation in **3** and **3′**, which results in the large GEO values. The average bond numbers of **3** [1.367] and **3′** [1.388] are smaller than that of benzene **1** [1.533] and borazine **2** [1.582], which leads to the increased EN values of **3** and **3′**. The bond numbers of **4′** show B–B single bond [0.950] and B–N multiple bond [1.437] characters, suggesting that the π electrons are relatively localized on each B–N–B unit. The average of the bond number of **4′** [1.275] is smaller than other systems, in agreement with the relatively large EN value.

Secondly, as an electronic criterion, the ELF and PDI values have been computed.[50–55] The calculated average ELF values together with its σ- and π-contributions and PDI values are listed in Table 1,[56–58] and the ELF isosurfaces at the bifurcation points of the σ and π systems are depicted in Fig. 3.[59] The ELF_{ave} values increase in the order **2** < **3′** < **4′** < **1**, from 0.56 for **2** to 0.81 for **1**, and the ELF_{π} values are found to be larger than the ELF_{σ} values for all molecules. The ELF_{π} values greater than 0.70 indicate that all molecules may have some aromatic character.[60] Benzene **1** shows the high ELF_{π} value of 0.91, in line with the pronounced aromatic nature. Borazine **2** presents an ELF_{π} value of 0.72 lower than that of benzene **1**, implying the less aromatic character. In contrast to highly symmetric benzene **1** (D_{6h}) and borazine **2** (D_{3h}), the B_4N_2 systems with the lower symmetry exhibit several distinguishable ELF_{π} values. For the neutral B_4N_2 system **3′**, the separations at the $(H_3P)B$–N bonds, HB–N bonds, and B–B bonds occur at the ELF_{π} values of 0.68, 0.82, and 0.94, respectively. The dianionic B_4N_2 system **4′** shows the first separation at the B–N bonds with a relatively high ELF_{π}-value of 0.75 and the B–B bonds are split at a significantly higher ELF_{π} value of 0.92. The average ELF_{π} values of 0.81 for **3′** and 0.81 for **4′** are between those of benzene **1** (0.91) and borazine **2** (0.72), indicating moderate delocalization of π-electrons in those B_4N_2 systems.

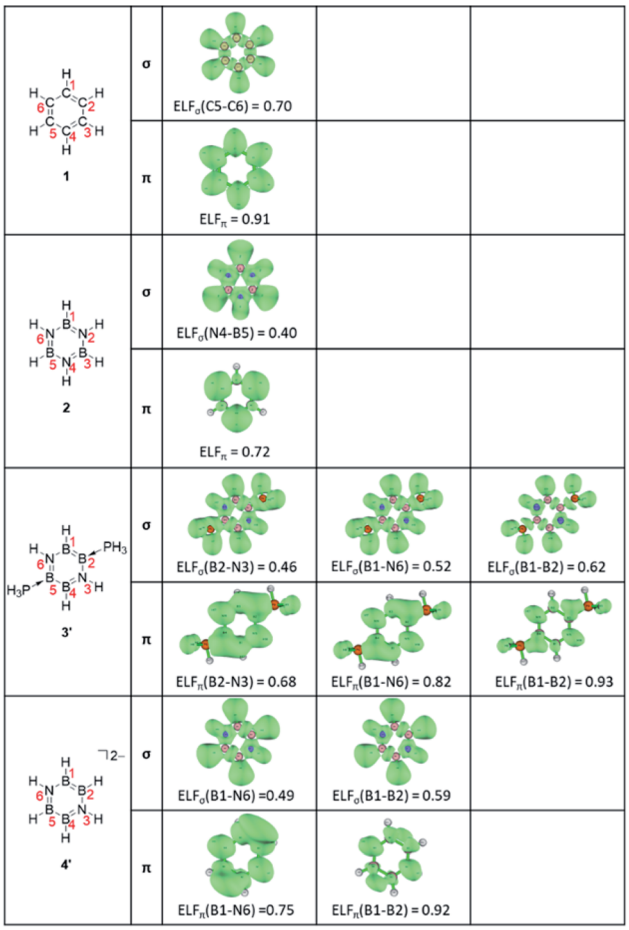

Fig. 3 The ELF isosurfaces at the bifurcation points of the σ and π systems of **1**, **2**, **3′**, and **4′**.

The ELF_{σ} values of inorganic benzenes [**2** (0.40), **3′** (0.47), **4′** (0.50)] are much smaller than that of benzene **1** (0.70), reflecting the difference of electronegativity between B and N atoms. The PDI values increase in the order **2** (0.041) < **3** (0.068) < **3′** (0.078) < **1** (0.105) < **4** (0.118), suggesting the moderate aromaticity of **3**

Table 1 Calculated HOMA, bifurcation values of ELF functions and PDI (electrons) values

	HOMA	EN	GEO	ELF_{ave}	ELF_{π}	ELF_{σ}	PDI
1: $(CH)_6$	0.990	0.010	0.000	0.81	0.91	0.70	0.105
2: $(HBNH)_3$	1.000	0.000	0.000	0.56	0.72	0.40	0.041
3: $[(MesN)(BCl)(BPMe_3)]_2$	0.698	0.189	0.113	—	—	—	0.068
3′: $[(HN)(BH)(BPH_3)]_2$	0.654	0.163	0.183	0.64	0.81	0.47	0.078
4′: $[(HN)_2(BH)_4]^{2-}$	0.288	0.428	0.284	0.66	0.81	0.50	0.118

Table 2 Calculated NICS values (ppm)

	$NICS_{zz}$		$NICS_{\pi zz}$		FiPC
Distance (Å)	0	1	0	1	—
1: $(CH)_6$	−14.48	−29.25	−35.78	−29.07	−9.07
2: $(HBNH)_3$	11.98	−5.17	−7.89	−5.88	−2.34
3: $[(MesN)(BCl)(BPMe_3)]_2$	−3.36	−12.32	—	—	−4.03
3′: $[(HN)(BH)(BPH_3)]_2$	−3.75	−15.18	−19.73	−16.54	−3.85
4′: $[(HN)_2(BH)_4]^{2-}$	−5.49	−15.42	−20.73	−17.02	—

and **3′**, which is in agreement with the ELF_π values. However, the PDI value of **4** greater than that of benzene **1**, as inconsistent with those ELF_π values, points out that the PDI measures might not be suitable for the evaluation of the relative aromaticity among the differently charged molecules, as well as, compounds consisting of different skeletal atoms.[61,62] The calculated ring critical point properties of compounds **1**, **2**, **3**, **3′**, **4′** are summarized in Table S4.†

Thirdly, as a magnetic criterion, a series of NICS values have been estimated (Table 2).[63–68] Isotropic NICS can be represented by the anisotropic components: $NICS = (NICS_{xx} + NICS_{yy} + NICS_{zz})/3 = NICS_{in\text{-}plane} + NICS_{out\text{-}of\text{-}plane}$, in which $(NICS_{xx} + NICS_{yy})/3 = (NICS_{in\text{-}plane})$ and $(NICS_{zz})/3 = NICS_{out\text{-}of\text{-}plane}$. Free of in-plane component NICS (FiPC-NICS) indicates the NICS value at a point above the molecular ring with zero of $NICS_{in\text{-}plane}$. Fig. 4(a) presents the NICS-profiles of the full-$NICS_{zz}$ and σ- and π-electron contribution to the $NICS_{zz}$ for **3′** and **4′**, from the center of the six-membered ring and above up to 5.00 Å, and Fig. 4(b) shows FiPC-NICS plot, respectively.

While the $NICS_{zz}(0)$ values of **1** (−14.48), **3** (−3.36), **3′** (−3.75), and **4′** (−5.49) are negative, borazine **2** shows the highly positive $NICS_{zz}(0)$ values of 11.98, which is due to the significantly positive $NICS_{\sigma zz}(0)$ contribution.[66] It has been demonstrated that $NICS_{\pi zz}$ in addition to $NICS_{zz}(1)$ could be the most reliable aromaticity indexes, with statistically good correlation with aromatic stabilization energies.[64,69] The $NICS_{zz}$ values of **3** [$NICS_{zz}(1) = -12.32$], **3′** [$NICS_{zz}(1) = -15.18$, $NICS_{\pi zz}(0) = -19.73$, $NICS_{\pi zz}(1) = -16.54$] and **4′** [$NICS_{zz}(1) = -15.42$, $NICS_{\pi zz}(0) = -20.73$, $NICS_{\pi zz}(1) = -17.02$] lie in between those of benzene **1** [$NICS_{zz}(1) = -29.25$, $NICS_{\pi zz}(0) = -35.78$, $NICS_{\pi zz}(1) = -29.07$] and borazine **2** [$NICS_{zz}(1) = -5.17$, $NICS_{\pi zz}(0) = -7.89$, $NICS_{\pi zz}(1) = -5.88$].

The $NICS_{zz}$ profiles of **3′** and **4′** (Fig. 4(a)) confirm that the $NICS_{\sigma zz}$ values are significantly positive near the ring center [$NICS_{\sigma zz}(0) = 15.98$ (**3′**), 15.25 (**4′**)], and they decrease as being apart from the ring and become negative around at 1 Å. On the other hand, the $NICS_{\pi zz}$ values are significantly negative at the molecular center, and gradually become less negative as being away from the ring. The greatly negative $NICS_{\pi zz}$ contribution over the $NICS_{\sigma zz}$ component leads to the overall negative $NICS_{zz}$ values. A similar trend of the $NICS_{zz}$ profile is found for benzene.[66] The FiPC-NICS value corresponds to the interception on the vertical axis ($NICS_{out\text{-}of\text{-}plane}$) in Fig. 4(b). The FiPC-NICS values of −4.03 for **3** and −3.85 for **3′**, appear to be between those of benzene **1** (−9.07) and borazine **2** (−2.34), supporting the moderate aromatic character of **3** and **3′**. The shape of FiPC-NICS plots of **3** and **3′** is similar

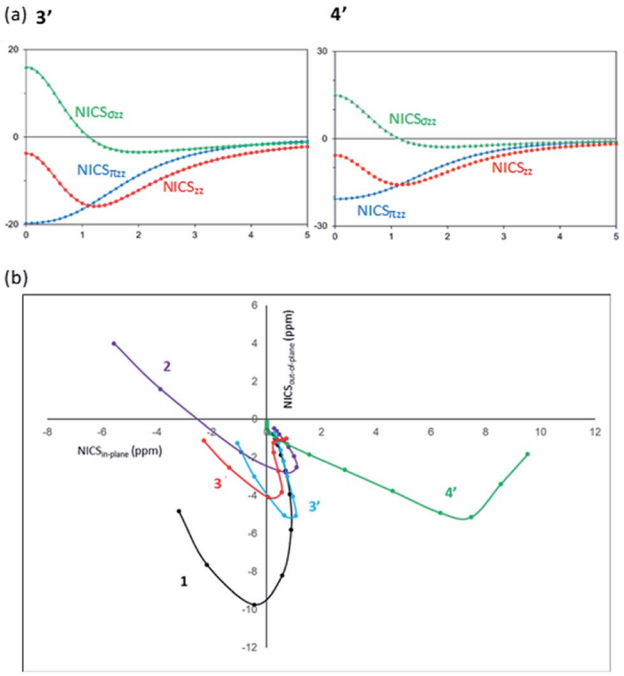

Fig. 4 (a) Dissected $NICS_{zz}$ (ppm) *vs.* distance (Å) of **3′** and **4′**. (b) Plots of the $NICS_{in\text{-}plane}$ *vs.* $NICS_{out\text{-}of\text{-}plane}$ of **1**, **2**, **3**, **3′** and **4′**, to identify the FiPC-NICS.

to that of **1** but different from that of **2**. The positive $NICS_{out\text{-}of\text{-}plane}$ values are observed near the ring center of **2**, which is due to the pronounced σ-contribution but marginal π-contribution in the region.[66] The significant deviation of the FiPC-NICS plot of **4′** from others can be rationalized by the largely positive $NICS_{xx}$ values, and therefore, the FiPC-NICS value of **4′** could not be gained.

ACID plot of **4′** is shown in Fig. 5 (For the plots of **1**, **2**, **3′**, see Fig. S1†). While the clear clockwise current–density vectors are confirmed on the ACID isosurface of benzene **1**, borazine **2** shows the imperceptible ring current consisting of the three localized circulations on the nitrogen atoms, which is consistent with previous studies.[24] The clockwise current–density vectors on the ACID isosurface also observed in **3**.[27] Despite somehow weak vectors, an explicit diatropic ring current is seen over the B_4N_2 ring of **4′** with the pronounced stopover at the B–H moieties.

Finally, an energetic criterion is evaluated using the ASE method (Table 3). The ASE values computed by the reactions (a)–(d) (Scheme 2, Table S5–S8†)[65,70] decrease in the order **1**

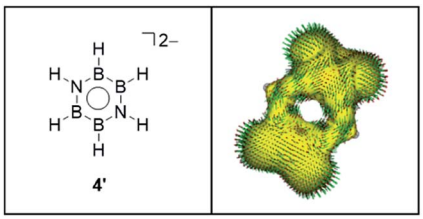

Fig. 5 ACID plot of the selected π orbitals of **4′**, at an isosurface value of 0.03.

Table 3 Calculated ASE values (kcal mol^{-1})

	ASE
1: $(CH)_6$	33.4 (100)
2: $(HBNH)_3$	10.1 (30)
3: $[(MesN)(BCl)(BPMe_3)]_2$	—
3′: $[(HN)(BH)(BPH_3)]_2$	23.8 (71)
4′: $[(HN)_2(BH)_4]^{2-}$	11.0 (33)

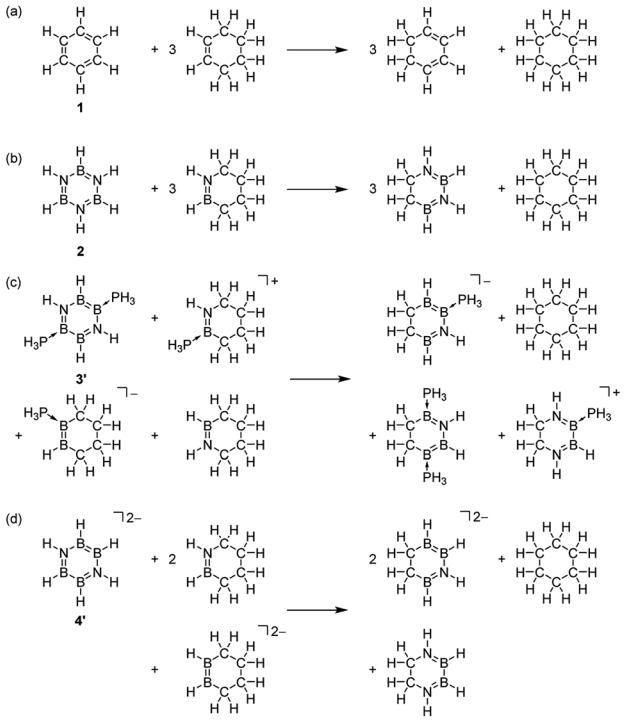

Scheme 2 Homodesmotic reaction schemes used to estimate the aromatic stabilization energy (ASE).

(33.4 kcal mol^{-1}) > **3′** (23.8 kcal mol^{-1}) > **4′** (11.0 kcal mol^{-1}) > **2** (10.1 kcal mol^{-1}). Based on the ASE values, it can be estimated that inorganic benzene analogues **2**, **3′**, **4′** present 30%, 71% and 33% of aromaticity in comparison to benzene, respectively. Note that the significantly smaller ASE value of **4′** compared with that of **3′** is not in line with those $NICS_{\pi zz}(0)$ values [**3′** = −19.73; **4′** = −20.73], indicating that magnetic and energetic criteria are not in good correlation with each other when comparing the differently charged molecules.[64]

Conclusions

In conclusion, we have assessed the aromatics-relevant indices of B_4N_2-based inorganic benzene analogues together with benzene and borazine, with the aid of HOMA, ELF, PDI, NICS, ACID and ASE methods. It has been demonstrated that the aromaticity of the neutral B_4N_2 systems **3** and **3′** clearly differs from that of borazine **2** of the $(XY)_3$ system. The major parameters (ELF, PDI, $NICS_{zz}$, and ASE) other than HOMA suggest that the neutral B_4N_2 systems **3** and **3′** are less aromatic than benzene and more aromatic than borazine **2**. While ELF_{π}, PDI and $NICS_{\pi zz}$ values propose the pronounced aromatic nature of the dianionic B_4N_2 system **4′**, the ASE result estimates the aromaticity of **4′** to be smaller than that of **3′** and similar to borazine **2**. Moreover, the FiPC-NICS plot of **4′** is different from those observed for the aromatic molecules.[65] Besides, ACID plot of **4′** shows that in addition to the ring current over the six-membered ring, localized currents in the RB-BH fragment significantly contributes to magnetic anisotropy. These data indicate that even with the same B_4N_2-skeletal framework of 6π-system, the index value of each criterion varies depending on the overall charge of the B_4N_2 systems,[32,33,36] giving rise to the different aromatic nature.[71,72] This study paves a way for the further design and development of aromatic inorganic benzenes.

Conflicts of interest

There are no conflicts to declare.

Acknowledgements

This work was financially supported by Nanyang Technological University (NTU), Singapore, and the Singapore Ministry of Education (MOE2018-T2-2-048(S)) for R. K. We thank Mr S. H. J. Melvin (NTU) for assistance in the calculation.

Notes and references

1 P. R. v. Schleyer and J. Haijun, *Pure Appl. Chem.*, 1996, **68**, 209–218.
2 P. v. R. Schleyer, *Chem. Rev.*, 2001, **101**, 1115–1118.
3 A. T. Balaban, P. v. R. Schleyer and H. S. Rzepa, *Chem. Rev.*, 2005, **105**, 3436–3447.
4 M. Faraday, *Phil. Trans. R. Soc. Lond.*, 1825, **115**, 440–466.
5 A. Kekulé, *Bull. Soc. Chim. Fr.*, 1865, **3**, 98–110.
6 K. Ota and R. Kinjo, *Chem.–Asian J.*, 2020, **15**, 2558–2574.
7 A. Stock and E. Pohland, *Ber. Dtsch. Chem. Ges.*, 1926, **59**, 2215–2223.
8 H. R. Allcock, *Chem. Rev.*, 1972, **72**, 315–356.
9 A. L. Korich and P. M. Iovine, *Dalton Trans.*, 2010, **39**, 1423–1431.
10 Y. Tokunaga, *Heterocycles*, 2013, **87**, 991–1021.
11 E. W. David, *US*, US3035095A, 1962.
12 H. V. R. Dias and P. P. Power, *Angew. Chem., Int. Ed. Engl.*, 1987, **26**, 1270–1271.
13 H. V. R. Dias and P. P. Power, *J. Am. Chem. Soc.*, 1989, **111**, 144–148.
14 P. P. Power, *J. Organomet. Chem.*, 1990, **400**, 49–69.
15 A. E. Seitz, M. Eckhardt, A. Erlebach, E. V. Peresypkina, M. Sierka and M. Scheer, *J. Am. Chem. Soc.*, 2016, **138**, 10433–10436.
16 W. H. Fink and J. C. Richards, *J. Am. Chem. Soc.*, 1991, **113**, 3393–3398.

17 P. v. R. Schleyer, H. Jiao, N. J. R. v. E. Hommes, V. G. Malkin and O. L. Malkina, *J. Am. Chem. Soc.*, 1997, **119**, 12669–12670.
18 E. D. Jemmis and B. Kiran, *Inorg. Chem.*, 1998, **37**, 2110–2116.
19 J. J. Engelberts, R. W. A. Havenith, J. H. van Lenthe, L. W. Jenneskens and P. W. Fowler, *Inorg. Chem.*, 2005, **44**, 5266–5272.
20 A. K. Phukan, A. K. Guha and B. Silvi, *Dalton Trans.*, 2010, **39**, 4126–4137.
21 R. Pino-Rios, A. Vásquez-Espinal, L. Alvarez-Thon and W. Tiznado, *Phys. Chem. Chem. Phys.*, 2020, **22**, 22973–22978.
22 P. W. Fowler and E. Steiner, *J. Phys. Chem. A*, 1997, **101**, 1409–1413.
23 A. Y. Timoshkin and G. Frenking, *Inorg. Chem.*, 2003, **42**, 60–69.
24 R. Islas, E. Chamorro, J. Robles, T. Heine, J. C. Santos and G. Merino, *Struct. Chem.*, 2007, **18**, 833–839.
25 R. Ghiasi, *J. Mol. Struct.*, 2008, **853**, 77–81.
26 S. Pelloni, G. Monaco, P. Lazzeretti and R. Zanasi, *Phys. Chem. Chem. Phys.*, 2011, **13**, 20666–20672.
27 K. Ota and R. Kinjo, *Angew. Chem., Int. Ed.*, 2020, **59**, 6572–6575.
28 B. Su, K. Ota, K. Xu, H. Hirao and R. Kinjo, *J. Am. Chem. Soc.*, 2018, **140**, 11921–11925.
29 M. Solà, *Front. Chem.*, 2017, **5**, 22.
30 J. T. Nelson and W. J. Pietro, *Inorg. Chem.*, 1989, **28**, 544–548.
31 T. M. Krygowski, K. Ejsmont, B. T. Stepień, M. K. Cyrański, J. Poater and M. Solà, *J. Org. Chem.*, 2004, **69**, 6634–6640.
32 R. Miao, G. Yang, C. Zhao, J. Hong and L. Zhu, *J. Mol. Struct.*, 2005, **728**, 197–202.
33 M. Baranac-Stojanović and M. Stojanović, *RSC Adv.*, 2013, **3**, 24108–24117.
34 A. K. Srivastava, S. K. Pandey and N. Misra, *Theor. Chem. Acc.*, 2016, **135**, 158.
35 A. K. Srivastava, S. K. Pandey and N. Misra, *Mol. Phys.*, 2016, **114**, 1763–1770.
36 W. A. Rabanal-León, W. Tiznado and L. Alvarez-Thon, *Int. J. Quantum Chem.*, 2019, **119**, e25859.
37 M. J. Frisch, G. W. Trucks, H. B. Schlegel, G. E. Scuseria, M. A. Robb, J. R. Cheeseman, G. Scalmani, V. Barone, G. A. Petersson, H. Nakatsuji, X. Li, M. Caricato, A. V. Marenich, J. Bloino, B. G. Janesko, R. Gomperts, B. Mennucci, H. P. Hratchian, J. V. Ortiz, A. F. Izmaylov, J. L. Sonnenberg, D. Williams-Young, F. Ding, F. Lipparini, F. Egidi, J. Goings, B. Peng, A. Petrone, T. Henderson, D. Ranasinghe, V. G. Zakrzewski, J. Gao, N. Rega, G. Zheng, W. Liang, M. Hada, M. Ehara, K. Toyota, R. Fukuda, J. Hasegawa, M. Ishida, T. Nakajima, Y. Honda, O. Kitao, H. Nakai, T. Vreven, K. Throssell, J. A. Montgomery Jr, J. E. Peralta, F. Ogliaro, M. J. Bearpark, J. J. Heyd, E. N. Brothers, K. N. Kudin, V. N. Staroverov, T. A. Keith, R. Kobayashi, J. Normand, K. Raghavachari, A. P. Rendell, J. C. Burant, S. S. Iyengar, J. Tomasi, M. Cossi, J. M. Millam, M. Klene, C. Adamo, R. Cammi, J. W. Ochterski, R. L. Martin, K. Morokuma, O. Farkas, J. B. Foresman and D. J. Fox, *Gaussian 16*, Gaussian, Inc., Wallingford, CT, 2016.
38 M. Baranac-Stojanović, *Chem.–Eur. J.*, 2014, **20**, 16558–16565.
39 M. Stojanović and M. Baranac-Stojanović, *J. Org. Chem.*, 2016, **81**, 197–205.
40 R. A. Iwaki and T. Udagawa, *Chem. Phys. Lett.*, 2020, **745**, 137271–137275.
41 E. D. Glendening, J. K. Badenhoop, A. E. Reed, J. E. Carpenter, J. A. Bohmann, C. M. Morales, P. Karafiloglou, C. R. Landis and F. Weinhold, *NBO 7.0.*, Theoretical Chemistry Institute, University of Wisconsin, Madison, 2018.
42 T. Lu and F. Chen, *J. Comput. Chem.*, 2012, **33**, 580–592.
43 A. Julg and P. François, *Theor. Chim. Acta*, 1967, **8**, 249–259.
44 J. Kruszewski and T. M. Krygowski, *Tetrahedron Lett.*, 1972, **13**, 3839–3842.
45 T. M. Krygowski, *J. Chem. Inf. Comput. Sci.*, 1993, **33**, 70–78.
46 T. M. Krygowski and M. Cyrański, *Tetrahedron*, 1996, **52**, 1713–1722.
47 T. M. Krygowski and M. Cyrański, *Tetrahedron*, 1996, **52**, 10255–10264.
48 I. D. Madura, T. M. Krygowski and M. K. Cyrański, *Tetrahedron*, 1998, **54**, 14913–14918.
49 K. K. Zborowski, I. Alkorta, J. Elguero and L. M. Proniewicz, *Struct. Chem.*, 2013, **24**, 543–548.
50 A. D. Becke and K. E. Edgecombe, *J. Chem. Phys.*, 1990, **92**, 5397–5403.
51 A. Savin, A. D. Becke, J. Flad, R. Nesper, H. Preuss and H. G. von Schnering, *Angew. Chem., Int. Ed. Engl.*, 1991, **30**, 409–412.
52 B. Silvi and A. Savin, *Nature*, 1994, **371**, 683–686.
53 A. Savin, R. Nesper, S. Wengert and T. F. Fässler, *Angew. Chem., Int. Ed. Engl.*, 1997, **36**, 1808–1832.
54 J. Poater, X. Fradera, M. Duran and M. Solà, *Chem. Eur. J.*, 2003, **9**, 400–406.
55 F. Feixas, E. Matito, J. Poater and M. Solà, *Chem. Soc. Rev.*, 2015, **44**, 6434–6451.
56 J. C. Santos, W. Tiznado, R. Contreras and P. Fuentealba, *J. Chem. Phys.*, 2004, **120**, 1670–1673.
57 J. C. Santos, J. Andres, A. Aizman and P. Fuentealba, *J. Chem. Theory Comput.*, 2005, **1**, 83–86.
58 J. Pilmé, *J. Comput. Chem.*, 2017, **38**, 204–210.
59 The calculated PDI value (0.041) is larger than that of reported values. We thought the calculated values are depends on the calculation level and software. ref: J. E. Del Bene, M. Yáñez, I. Alkorta and J. Elguero, *J. Chem. Theory Comput.*, 2009, **5**, 2239–2247; M. Baranac-Stojanović and M. Stojanović, *RSC Adv.*, 2013, **3**, 24108–24117.
60 M. Solà, *Aromaticity*, John Wiley & Sons, Ltd, 2017.
61 P. Bultinck, *Faraday Discuss.*, 2007, **135**, 347–365.
62 F. Feixas, E. Matito, J. Poater and M. Solà, *J. Comput. Chem.*, 2008, **29**, 1543–1554.
63 Z. Chen, C. S. Wannere, C. Corminboeuf, R. Puchta and P. v. R. Schleyer, *Chem. Rev.*, 2005, **105**, 3842–3888.
64 H. Fallah-Bagher-Shaidaei, C. S. Wannere, C. Corminboeuf, R. Puchta and P. v. R. Schleyer, *Org. Lett.*, 2006, **8**, 863–866.

65 J. J. Torres-Vega, A. Vásquez-Espinal, J. Caballero, M. L. Valenzuela, L. Alvarez-Thon, E. Osorio and W. Tiznado, *Inorg. Chem.*, 2014, **53**, 3579–3585.
66 R. Báez-Grez, L. Ruiz, R. Pino-Rios and W. Tiznado, *RSC Adv.*, 2018, **8**, 13446–13453.
67 A. Stanger, *Eur. J. Org. Chem.*, 2020, **2020**, 3120–3127.
68 R. Gershoni-Poranne and A. Stanger, *Chem. Soc. Rev.*, 2015, **44**, 6597–6615.
69 R. Báez-Grez, W. A. Rabanal-León, L. Alvarez-Thon, L. Ruiz, W. Tiznado and R. Pino-Rios, *J. Phys. Org. Chem.*, 2019, **32**, e3823.
70 E. Osorio, J. K. Olson, W. Tiznado and A. I. Boldyrev, *Chem. Eur. J.*, 2012, **18**, 9677–9681.
71 P. C. Parambil and R. Hoffmann, *J. Am. Chem. Soc.*, 2018, **140**, 12844–12852.
72 P. C. Parambil and S. S. R. R. Perumal, *Organometallics*, 2020, **39**, 2951–2955.